



# The origin of *n*-alkanes in Santa Monica Basin surface sediment: a model based on compound-specific $\Delta^{14}\text{C}$ and $\delta^{13}\text{C}$ data

A. Pearson\*, T.I. Eglinton

*Department of Marine Chemistry and Geochemistry, Woods Hole Oceanographic Institution, Woods Hole, MA 02543, USA*

Received 16 February 2000; accepted 17 August 2000  
(returned to author for revision 24 April 2000)

## Abstract

$\Delta^{14}\text{C}$  and  $\delta^{13}\text{C}$  values were measured for individual long-chain *n*-alkanes ( $\text{C}_{24-33}$ ) from Santa Monica Basin sediments. The data were then simulated using a three-component mixing model designed to represent the contributions of different sources. The three selected end members were petroleum, modern plant wax, and shale-derived alkanes. The model was optimized to fit the data and to determine the fractional contribution of each component. The results indicated that petroleum accounted for 12% of the alkanes in 0–2.5 cm sediment and 5% in 2.5–7.5 cm sediment. Modern plant waxes contributed 80% (0–2.5 cm) and 87% (2.5–7.5 cm), and the remaining 8% of each sample was attributed to the shale source. The  $^{14}\text{C}$  concentration of the modern terrestrial end member was also determined from the model.  $\Delta^{14}\text{C}$  values of  $\sim +235\text{‰}$  for the 0–2.5 cm (post-bomb) horizon and  $\sim 0\text{‰}$  for the 2.5–7.5 cm (pre-bomb) horizon indicate that plant leaf waxes have a continental residence time of decades in the southern California region. © 2000 Elsevier Science Ltd. All rights reserved.

*Keywords:* Carbon isotopes; Radiocarbon; *n*-Alkanes; Santa Monica Basin; Sediments

## 1. Introduction

Normal alkanes are ubiquitous in marine sediments, and their concentration distributions are frequently used to assess the relative inputs of terrestrial and autochthonous organic carbon (e.g. Gagosian et al., 1981; Schneider and Gagosian, 1985; Prahel et al., 1989). In thermally immature samples, a strong odd-even predominance usually is observed within the long-chain (*n*- $\text{C}_{24-35}$ ) homologues. Epicuticular leaf waxes of higher plants generally have a higher carbon preference index (CPI = 4–40; Collister et al., 1994a) than sediments in which these terrestrial products are presumed to be the dominant wax input (Tissot and Welte, 1984). Therefore, additional sources having lower CPI values must also contribute normal alkanes. Primary candidates

include petroleum, petroleum source rocks, and exposed continental rocks of intermediate thermal maturity (Brassell and Eglinton, 1980). The fractional contributions of these components are difficult to decouple from the terrestrial waxes under most circumstances, and various approaches have been tried (e.g. Collister et al., 1994b; Prahel et al., 1994).

Compound-specific isotopic analysis of individual biomarker lipids is a valuable tool to determine the sources of organic matter in marine sediments. This approach is well-established both for  $^{13}\text{C}$  (e.g. Hayes et al., 1990), and more recently, for  $^{14}\text{C}$  (Eglinton et al., 1997). In addition to serving as carbon source tracers, compound-specific  $^{14}\text{C}$  measurements can provide direct information about the residence time of carbon in global reservoirs, and reveal the presence of fossil carbon input or contamination. In this work we build on previous approaches used to model the origin of normal hydrocarbons derived from multiple end member sources (Collister et al., 1994a,b; Lichtfouse and Eglinton,

\* Corresponding author.

E-mail address: apearson@whoi.edu (A. Pearson).

1996). Here we combine a set of coupled  $\Delta^{14}\text{C}$  and  $\delta^{13}\text{C}$  measurements for individual, long-chain *n*-alkanes extracted from Santa Monica Basin (SMB) sediments. An algebraic model is then employed to decouple the fossil and modern terrestrial plant wax components. In addition, the model supplies an estimate of the continental residence time of non-fossil, vascular plant-derived carbon.

SMB has a high sedimentation rate, and its suboxic bottom waters inhibit bioturbation. As a result, laminated cores recovered from the basin depocenter allow decadal resolution of recent changes in the  $^{14}\text{C}$  record. “Bomb- $^{14}\text{C}$ ” produced by atmospheric weapons testing is deposited in SMB sediments through the uptake of  $^{14}\text{CO}_2$  by primary producers, both terrestrial and marine, and subsequent sedimentation of their organic detritus. Thus, this record provides constraints on the timing of carbon fixation and its transfer between terrestrial and marine reservoirs. In this study, the sediments were divided into “pre-bomb” and “post-bomb” horizons. Further resolution was limited by the low abundance of individual alkanes in these samples.

## 2. Methods

### 2.1. Samples

Samples were collected in November 1996 (R/V Roger Revelle, cruise Pulse-32) from the central Santa Monica Basin ( $33^\circ 44.0' \text{N}$ ,  $118^\circ 50.0' \text{W}$ ), CA, USA. Seven sub-cores from one deployment (central basin, 905 m) of an Ocean Instruments<sup>®</sup> Multicorer were sectioned at 0.75-cm intervals to 1.5 cm and then 1.0-cm intervals to 7.5 cm. Measurements of excess  $^{210}\text{Pb}$  and  $\Delta^{14}\text{C}$  of total organic carbon (Pearson et al., 2000) indicated the 0–2.5 cm horizons were deposited after AD 1960 and contained  $^{14}\text{C}$  from atmospheric nuclear weapons testing. These horizons were combined into a single, “post-bomb” sample for alkane analysis. The 2.5–7.5 cm horizons were combined into a “pre-bomb” (prior to 1960) sample.

### 2.2. Lipid analysis

Freeze-dried sediments were extracted with 93:7  $\text{CH}_2\text{Cl}_2/\text{CH}_3\text{OH}$  (Fisher GC Resolv<sup>®</sup> or Burdick & Jackson GC<sup>2</sup>) using a large Soxhlet apparatus. The total lipid extracts (TLE) were transesterified, and the lipids were partitioned into hexane (Fisher GC Resolv<sup>®</sup>; 8 × 30 ml). Hexane extracts were dried onto quartz sand and separated into 10 fractions on a Biotage<sup>®</sup> Flash 40Mi pressurized chromatography system (column: 15 cm × 40 mm,  $\text{SiO}_2$ -gel, 32–63  $\mu\text{m}$ ) equipped with a solid-phase sample introduction module. Normal alkanes eluted in the first fraction (100% hexane), which was split for

$\delta^{13}\text{C}$  (5%) and  $\Delta^{14}\text{C}$  (95%) analysis. Blank analyses of concentrated solvents and flash chromatography fractions yielded unmeasurable or insignificant quantities of *n*-alkanes.

The *n*-alkanes for isotopic analysis were separated from the unresolved complex mixture (UCM) by urea adduction. Non-adducts were separated by rinsing the urea crystals with *iso*-octane. Adducted *n*-alkanes (and *n*-alkenes) were partitioned into hexane after addition of  $\text{H}_2\text{O}$  to dissolve the urea crystals. The samples were eluted through acid-cleaned granular Cu to remove elemental sulfur; then they were passed through a mini-column packed with  $\text{AgNO}_3$ -impregnated  $\text{SiO}_2$  gel to remove *n*-alkenes, leaving *n*-alkanes for isotopic analysis.

### 2.3. High-resolution gas chromatography (HRGC)

Routine gas chromatography (GC) was performed on a HP 5890 Series II GC equipped with a Gerstel CIS-3 injector, and dual columns and FID detectors. Capillary columns were J&W Scientific DB-5 and Chrompack CP-Sil 5CB, both 60 m × 0.32 mm × 0.25  $\mu\text{m}$ . Samples were run using constant flow mode (He carrier gas), and the temperature program was 40°C (1 min), 4°C/min to 320°C (35 min).

### 2.4. Gas chromatography mass spectrometry (GC/MS)

*n*-Alkane identities were confirmed on a high-resolution mass spectrometer (VG Autospec-Q hybrid MS; EI ionization energy, 70 eV) interfaced with a HP 5890 Series II GC. A J&W Scientific DB-5 column (60 m × 0.32 mm × 0.25  $\mu\text{m}$ ) was used, and GC conditions were as stated above.

### 2.5. Isotope ratio monitoring gas chromatography mass spectrometry (irm-GC/MS)

Compound-specific  $\delta^{13}\text{C}$  values were determined in triplicate on a Finnigan Delta<sup>Plus</sup> stable isotope mass spectrometer with attached Finnigan GC combustion III interface and HP 6890 GC, configured similarly to the system described in Hayes et al. (1990). Samples were injected via cool on-column injection and separated on a J&W Scientific DB-5MS (60 m × 0.25 mm × 25  $\mu\text{m}$ ) column equipped with a 1-m deactivated silica guard column. Isotope ratios for all peaks were calculated relative to multiple pulses of  $\text{CO}_2$  reference gas. The standard deviations of the replicate measurements are reported individually for each peak, and are generally  $< \pm 0.4\%$ . Accuracy was also checked by separate measurement of a series of *n*-alkanes of known isotopic composition ( $\text{C}_{24}$ ,  $\text{C}_{32}$ ,  $\text{C}_{34}$ , and  $\text{C}_{40}$ ; obtained from the laboratory of J.M. Hayes).  $\delta^{13}\text{C}$  is reported relative to the VPDB standard.

## 2.6. Preparative capillary gas chromatography (PCGC)

Collection of microgram quantities of purified individual lipids by PCGC was described in detail by Eglinton et al. (1996). A HP 5890 series II GC, equipped with HP 7673 auto-injector, Gerstel CIS-3 injection system, and Gerstel preparative trapping device (PTD) was fitted with a Chrompak CP-Sil 5 CB column (100% dimethylpolysiloxane, 100 m×0.53 mm×0.5 µm). The CIS injection volume was 5 µl, and the GC temperature program was 40°C (1 min), 20°C/min to 160°C, 4°C/min to 320°C (25 min). One percent of the effluent passed to an FID and the remaining 99% was collected in a series of seven U-tube traps (room temperature). Computer control allowed synchronization of the trapping time windows, permitting collection of multiple identical runs (>100 consecutive injections). Four traps were programmed to collect compounds of interest, two were left empty, and the seventh (waste trap) received the remainder of the mixture. Trace amounts of column bleed (yellow color) migrated to the U-tubes during collection. This contaminant was removed by eluting the trap contents through SiO<sub>2</sub>-gel columns (prepared in Pasteur pipettes, then combusted at 450°C, 8 h) into pre-combusted quartz tubes (850°C, 5 h). The solvent (hexane) was evaporated under ultra-high-purity N<sub>2</sub>.

## 2.7. Accelerator mass spectrometry (AMS)

The purified samples from PCGC were evacuated, flame-sealed with 100 mg CuO, and combusted to CO<sub>2</sub> (850°C, 5 h). Sample yields ranged from 20–86 µgC. The CO<sub>2</sub> was reduced to graphite over cobalt catalyst (Pearson et al., 1998). <sup>14</sup>C-AMS analysis was performed using special methods (von Reden et al., 1998) necessary for the accurate determination of Δ<sup>14</sup>C in samples containing <0.5–1.0 mgC, the amount normally used for <sup>14</sup>C-AMS measurements. For our samples, which have known geochronological ages, the reported Δ<sup>14</sup>C = [ $f_m e^{(1950-x)\lambda} - 1$ ]/1000 (Stuiver and Polach, 1977), where λ = 1/8267 (year<sup>-1</sup>),  $f_m$  = fraction modern <sup>14</sup>C, corrected for isotopic fractionation using δ<sup>13</sup>C, and “x” equals the year of deposition (determined from the <sup>210</sup>Pb chronology). This removes the effects of in-situ <sup>14</sup>C decay, yielding the Δ<sup>14</sup>C values each sample had when deposited at the sediment–water interface.

## 3. Results

### 3.1. Alkane distribution

A chromatogram of the total aliphatic hydrocarbon fraction from SMB 0–2.5 cm (post-bomb) sediment is shown in Fig. 1a. The total mixture was characterized by the presence of an abundant unresolved complex

mixture (UCM) typical of samples containing degraded petroleum. Fig. 1b shows the same fraction following urea adduction and subsequent removal of alkenes by elution through AgNO<sub>3</sub>. The resulting sample for isotopic analysis contained a homologous series of *n*-alkanes, as well as minor amounts of simply-branched hydrocarbons that were not removed via urea adduction. Similar results were obtained for the SMB pre-bomb (2.5–7.5 cm) aliphatic hydrocarbon fraction (chromatogram not shown).

Fig. 2 shows the abundance of *n*-alkanes in each sample, relative to *n*-C<sub>29</sub>. In both surface and deeper sediments, the individual alkanes were present at concentrations of less than 1 µg/gdw. Therefore, to obtain sufficient sample yields for compound-specific <sup>14</sup>C analysis, it was necessary to study the core at coarse resolution by dividing into “pre-“ and “post-bomb” sections only. In both of these intervals, *n*-C<sub>29</sub> was the most abundant homologue, and the strong odd-even predominance is consistent with a significant contribution from terrestrial plant waxes. A simplified carbon preference index (CPI) calculation (C<sub>25+27+29+31+33</sub>)/ (C<sub>24+26+28+30+32</sub>) resulted in CPI = 3.8 for the surface sediments and CPI = 5.4 for the deeper horizon. The presence of homologues with chain length >C<sub>35</sub>, or longer than the typical plant wax series, was also indicative of a petroleum-derived component. Isotopic data are reported here only for the most abundant and easily analyzed compounds (C<sub>24–33</sub>; Table 1).

### 3.2. δ<sup>13</sup>C data

The distribution of <sup>13</sup>C was similar in both the SMB post-bomb (0–2.5 cm) and pre-bomb (2.5–7.5 cm) *n*-alkane fractions. In both cases, the even-chain homologues have δ<sup>13</sup>C values that are relatively more constant and more <sup>13</sup>C-enriched than the odd-chain isomers. The average δ<sup>13</sup>C for even-numbered compounds was –29.9‰ between 0 and 2.5 cm and –30.4‰ between 2.5 and 7.5 cm. These values were consistent with a predominantly petroleum source (e.g. Wilhelms et al., 1994). The isotopic depletion in the 2.5–7.5 cm sample probably reflects a slightly larger terrestrial plant contribution to the even-chain isomers in these horizons. The odd-chain *n*-alkanes in both intervals were characterized by a strong minimum in δ<sup>13</sup>C at *n*-C<sub>31</sub> with significant isotopic depletion also observed for *n*-C<sub>29</sub> and *n*-C<sub>33</sub>. Terrestrial C<sub>3</sub> plant waxes with typical δ<sup>13</sup>C values between –30 and –36‰ (Collister et al., 1994a; Bird et al., 1995; Lockheart et al., 1996) probably are the origin of this isotopic depletion. It is interesting, however, that the maximum concentration occurred at *n*-C<sub>29</sub> but the minimum δ<sup>13</sup>C occurred at *n*-C<sub>31</sub> in both intervals. The even- and odd-chain data together suggested there were multiple hydrocarbon sources with different <sup>13</sup>C isotopic compositions contributing to SMB sediment.

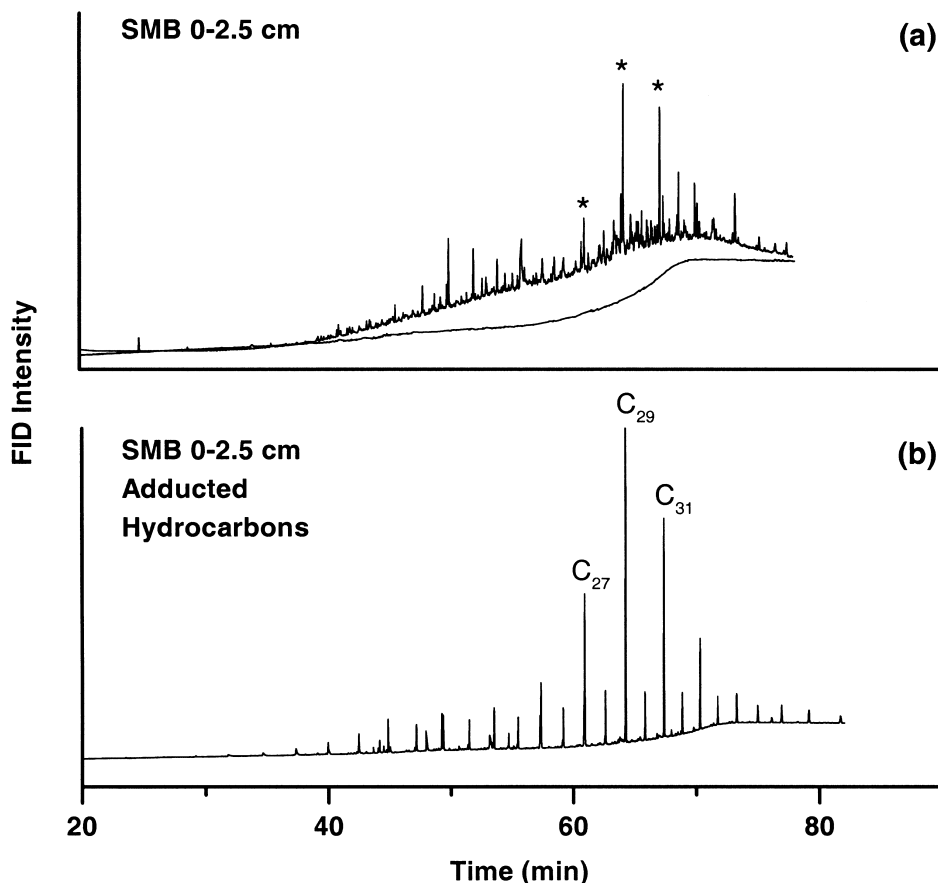


Fig. 1. (a) Total aliphatic hydrocarbon fraction for the SMB 0–2.5 cm sediment horizon; (b) *n*-alkane fraction obtained by urea adduction of the same sample.

### 3.3. $\delta^{14}\text{C}$ data

The  $\delta^{14}\text{C}$  values varied greatly for individual alkanes obtained from each homologous series. This variability is in strong contrast to the uniformity in  $^{14}\text{C}$  concentrations reported for sterols extracted from the same sediments ( $+62 \pm 23\%$  for surface sediment; Pearson et al., 2000). For pre- and post-bomb alkanes, the range of  $\delta^{14}\text{C}$  values observed was  $\sim 500$  and  $\sim 750\%$ , respectively. The pre-bomb (2.5–7.5 cm), odd-chain compounds had  $\delta^{14}\text{C}$  values between  $-223\%$  (*n*-C<sub>27</sub>) and  $-122\%$  (*n*-C<sub>29</sub>), while the composite sample of even-numbered *n*-alkanes (*n*-C<sub>24+26+28+30</sub>) was greatly depleted in  $^{14}\text{C}$  ( $-617\%$ ). The post-bomb (0–2.5 cm), odd-chain alkanes had a larger  $\delta^{14}\text{C}$  range than the pre-bomb samples,  $-243\%$  (*n*-C<sub>27</sub>) to  $+30\%$  (*n*-C<sub>29</sub>). The even-numbered homologues from the post-bomb sample were also strongly  $^{14}\text{C}$ -depleted ( $-741\%$ ).

The wide range of measured  $\delta^{14}\text{C}$  values is consistent with expectations based on the *n*-alkane concentration distributions. The even-numbered homologues appear

to be predominantly petroleum-derived. Values of  $-617$  and  $-741\%$  for even-chain *n*-alkanes correspond to  $\sim 62$  and  $\sim 74\%$  fossil carbon ( $\delta^{14}\text{C} = -1000\%$ ), respectively. The odd carbon-number alkanes also contain fossil components, but represent a higher proportion of material from modern plant waxes. The fraction derived from ancient and recent sources varies and results in the large spread in  $\delta^{14}\text{C}$  results for the C<sub>27</sub>, C<sub>29</sub>, and C<sub>31</sub> compounds. Perhaps the most informative value is the  $+30\%$  measurement obtained for *n*-C<sub>29</sub> from 0 to 2.5 cm. A positive  $\delta^{14}\text{C}$  value indicates that the quantitative majority of this compound in SMB sediment is of post-bomb origin and therefore less than 50 years old.

The changes in  $\delta^{14}\text{C}$  values between pre- and post-bomb samples also were not constant for the individual compounds. The data for *n*-C<sub>27</sub> and for the even-numbered homologues show that these lipids are more  $^{14}\text{C}$ -depleted in the post-bomb sediment than they are in the pre-bomb sediment. At least one component of the alkane series is of fossil origin, and the proportion of this component must be *greater* in the SMB 0–2.5 cm

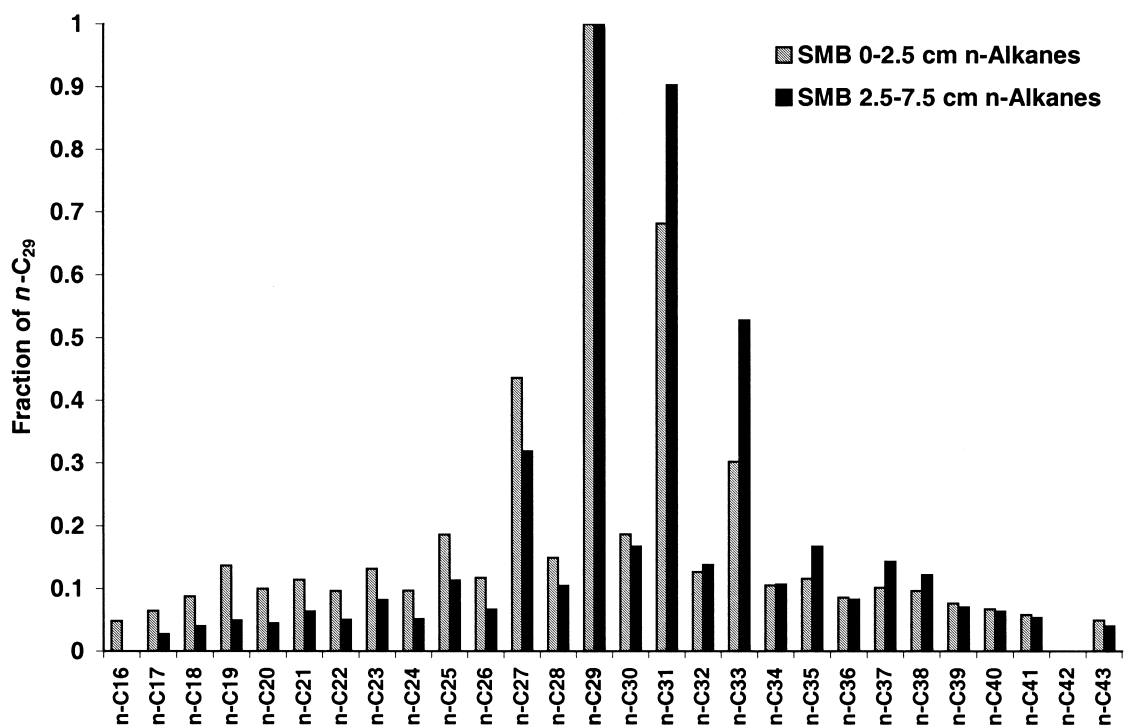


Fig. 2. Abundance of *n*-alkanes in SMB sediments relative to *n*-C<sub>29</sub>.

horizon than it is in the deeper sample. In contrast, the <sup>14</sup>C concentrations of *n*-C<sub>29</sub> and *n*-C<sub>31</sub> were higher in the surface sample, consistent with the presence of modern plant waxes influenced by bomb-<sup>14</sup>C uptake.

In the following section, we apply an algebraic mass balance model to explain these observations more quantitatively. The model uses the Δ<sup>14</sup>C and δ<sup>13</sup>C data to reconstruct both the isotopic signatures and the fractions of modern terrestrial and fossil carbon contributing to the total *n*-alkane distributions.

#### 4. Mixing model

The concentration distributions, δ<sup>13</sup>C values, and Δ<sup>14</sup>C values reported above are all consistent with the presence of two or more significant end member sources. SMB sediments receive hydrocarbons from both anthropogenic spills and natural petroleum seepage (Eganhouse and Venkatesan, 1993). Anthropogenic contributions derive from shipping activities, urban runoff, and deposition from nearby Los Angeles. Additional hydrocarbons may be contributed by weathering of outcrops of the Miocene Monterey Shale formation (Petsch et al., 2000; Schouten, 1995). Despite the importance of petroleum sources, the *n*-alkane distribution in both SMB sediment samples was more characteristic of higher plant waxes (Eglinton et al., 1962).

Terrestrial lipids may be preserved preferentially within the sediments, their flux may have decreased in recent years, or the flux of petroleum may have increased. The higher CPI in the deeper sediments is consistent with these hypotheses.

To assess these hypotheses quantitatively, we used an algebraic model based on the formula of Collister et al. (1994b) to predict the δ<sup>13</sup>C and Δ<sup>14</sup>C values for the entire set of measurements in Table 1. The model created by Collister et al. (1994b) was used to determine the relative contributions of different carbon sources to the alkanes of the Green River Formation, based on δ<sup>13</sup>C and concentration distributions only. Both δ<sup>13</sup>C and Δ<sup>14</sup>C data are used to constrain the version used here for SMB sediments. Our confidence in the model is correspondingly higher, because the fractional contribution of each end member must independently agree for both isotopes.

The notation for the model is based on the conventions of Collister (1992). It is also similar to the approach used by Lichtfouse and Eglinton (1996). The calculations for δ<sup>13</sup>C and Δ<sup>14</sup>C follow the analogous equations:

$$\delta^{13}C_{i,j} = \frac{\sum_k X_{i,k} W_{j,k} \delta^{13}C_{i,j,k}}{\sum_k X_{i,k} W_{j,k}}$$

and

Table 1  
SMB *n*-alkane isotopic data

<i>n</i> -Alkane	Pre-bomb (2.5–7.5 cm)		Post-bomb (0–2.5 cm)	
	$\delta^{13}\text{C}$ (‰)	$\Delta^{14}\text{C}$ (‰)	$\delta^{13}\text{C}$ (‰)	$\Delta^{14}\text{C}$ (‰)
<i>n</i> -C <sub>24</sub>	-30.2±0.1	-617±11 <sup>a</sup>	-29.2±0.4	-741±16 <sup>a</sup>
<i>n</i> -C <sub>25</sub>	-29.8±0.4		-30.2±0.1	
<i>n</i> -C <sub>26</sub>	-30.5±0.7		-30.0±0.4	
<i>n</i> -C <sub>27</sub>	-30.7±0.1	-223±17	-30.5±0.1	-243±20
<i>n</i> -C <sub>28</sub>	-30.5±0.4		-30.0±0.2	
<i>n</i> -C <sub>29</sub>	-31.9±0.1	-122±7	-31.3±0.2	+30±17
<i>n</i> -C <sub>30</sub>	-31.4±0.3		-30.3±0.4	
<i>n</i> -C <sub>31</sub>	-33.0±0.1	-170±15	-32.0±0.1	-113±19
<i>n</i> -C <sub>32</sub>	-30.9±0.2		-29.9±0.4	
<i>n</i> -C <sub>33</sub>	-32.5±0.3	i.s. <sup>b</sup>	-31.2±0.3	i.s.

<sup>a</sup>  $\Delta^{14}\text{C}$  for *n*-C<sub>24</sub>+<sub>26</sub>+<sub>28</sub>+<sub>30</sub> collected together as a single sample.

<sup>b</sup> Insufficient sample for analysis.

$$\Delta^{14}\text{C}_{i,j} = \sum_k X_{i,k} W_{j,k} \Delta^{14}\text{C}_{i,j,k} / \sum_k X_{i,k} W_{j,k}$$

The terms of the equations are defined as follows:

$W_{j,k}$  ≡ fraction of the carbon derived from source “*k*” in sample “*j*”.

$X_{i,k}$  ≡ fraction of the total *n*-alkane carbon in source “*k*” that belongs to alkane “*i*”, where all sources and samples are calculated in units of concentration relative to *n*-C<sub>29</sub>.

The product  $X_{i,k}W_{j,k}$  is the amount of carbon in alkane “*i*” contributed by source “*k*”, and the sum of these terms ( $\sum X_{i,k}W_{j,k}$ ) is the total concentration of a particular *n*-alkane. The fractional contributions,  $W$ , as well as the concentration distributions,  $X$  (e.g. CPI, weighting of *n*-C<sub>29</sub> or *n*-C<sub>31</sub>, etc.), were adjusted through iterations to produce the best possible agreement with the data.

$\delta^{13}\text{C}_{i,j,k}$  and  $\Delta^{14}\text{C}_{i,j,k}$  ≡ the isotopic composition of the portion of individual *n*-alkane, “*i*”, in sample “*j*”, that was derived from source “*k*”.

$\delta^{13}\text{C}_{i,j}$  and  $\Delta^{14}\text{C}_{i,j}$  ≡ the weighted average isotopic composition of *n*-alkane, “*i*”, in sample “*j*”. The model is calculated to maximize the agreement between these output values and the data.

The initial constraints on the model were chosen as follows:

- i. Concentration distribution: the *n*-alkanes were assumed to derive from three sources. Because studies of long-chain *n*-alkanes in marine organisms indicate they are minor components or perhaps merely analytical contamination (Sakata et al., 1997 and references therein), no marine end member was included in the model. A high-wax petroleum that had experienced some degradation of lower carbon-number alkanes was chosen as a

fossil carbon source (e.g. Lichtfouse and Eglinton, 1996). This oil was assumed to have CPI = 1, a maximum concentration around *n*-C<sub>26</sub> and *n*-C<sub>27</sub>, and a linear decrease in concentration, reaching zero abundance at *n*-C<sub>45</sub> (*n*-C<sub>43–45</sub> were the longest detectable chain lengths for SMB alkanes). Alkanes derived from a thermally immature weathered shale were also chosen as a second fossil end member. The concentration distribution for this source was estimated from the work of Schouten (1995) on the outcrops of the Monterey Shale. Free alkanes in these outcrops have an average CPI ~3, a maximum at *n*-C<sub>29</sub>, and are weighted toward *n*-C<sub>31</sub> rather than *n*-C<sub>27</sub>. The third end member was assumed to be the leaf waxes and degraded tissues of modern terrestrial plants. An arbitrary CPI ~10 with a concentration maximum at *n*-C<sub>29</sub> (and weighted toward *n*-C<sub>31</sub> rather than *n*-C<sub>27</sub>) was chosen for this end member. C<sub>29</sub> is the most abundant *n*-alkane in SMB sediments. High CPI numbers and concentration maxima at either C<sub>29</sub> or C<sub>31</sub> in marine sediments are typically due to the predominance of this plant wax source (e.g. Brassell and Eglinton, 1980; Volkman et al., 1980).

- ii.  $\delta^{13}\text{C}$  distribution: the petroleum end member was given a uniform value of -29.5‰. This value is approximately the same as the  $\delta^{13}\text{C}$  measured for *n*-C<sub>24</sub>, the compound believed to have the largest petroleum contribution among the C<sub>24–33</sub> isomers. Also,  $\delta^{13}\text{C}$  values within homologous series of fossil fuel alkanes usually are similar (Clayton and Bjorøy, 1994). The  $\delta^{13}\text{C}$  values chosen for the Monterey Shale end member varied for each compound and were based on the average  $\delta^{13}\text{C}$  measured for free *n*-alkanes from seven shale samples (Schouten, 1995). These numbers vary from ~-28‰ at *n*-C<sub>24–25</sub> to ~-32‰ at *n*-C<sub>31–33</sub>.

For both the petroleum and shale sources, the  $\delta^{13}\text{C}$  values were estimated only to  $\pm 0.5\%$  and were not adjusted in subsequent model iterations. The terrestrial *n*-alkane end member initially was given a uniform  $\delta^{13}\text{C} = -32\%$ . This value was chosen based on the  $\delta^{13}\text{C}$  of *n*-C<sub>29</sub>, the compound with the greatest terrestrial contribution. In subsequent iterations, the values for *n*-C<sub>31–33</sub> were decreased to  $-33\%$  to improve the agreement between the model and the data. Evidence for a trend toward lower  $\delta^{13}\text{C}$  values in plant species exhibiting higher average chain lengths (ACL = C<sub>31–33</sub>) has been found in some plants (Collister et al., 1994a; Reddy et al. 2000).

- iii.  $\Delta^{14}\text{C}$  distribution: by definition, the  $\Delta^{14}\text{C}$  of both fossil sources is  $-1000\%$ . In each of the pre-bomb and post-bomb sedimentary horizons, the terrestrial end member was assumed to have a uniform  $\Delta^{14}\text{C}$  for all *n*-alkanes. Therefore, only two values could be selected and manipulated, pre-bomb  $\Delta^{14}\text{C}_{\text{plantwax}}$  and post-bomb  $\Delta^{14}\text{C}_{\text{plantwax}}$ . The initial assumptions were 0 and  $+200\%$ , respectively. The final iteration of the model resulted in no change in the pre-bomb value (0%), while post-bomb  $\Delta^{14}\text{C}_{\text{plantwax}}$  achieved best agreement with the data when given a value of  $+235\%$ .

#### 4.1. Results

The data were simulated by mixing different fractions of the three end members: petroleum, shale, and modern plant wax. Very few iterations were needed before reaching good agreement between the calculated model and the data, and only minor adjustments were made to the initial parameters. The final results are summarized in Table 2. In both samples, the fraction of the alkanes derived from weathered shales is a constant 8%. The petroleum-derived fraction is greater in surface sediment than in pre-bomb sediment, consistent with the geo-

chemical data. However, the modern terrestrial end member dominates in both samples, representing 80 and 87% of the total (Fig. 3). In Fig. 3, the fractions of each end member contributing to the total modeled concentrations are shown. The post-bomb model and data agree within  $\sim 10\%$ , and the pre-bomb model and data agree nearly as well. The  $\sim 20\%$  errors for *n*-C<sub>31</sub> and *n*-C<sub>33</sub> in the pre-bomb sample are larger, perhaps, than the errors associated with GC-FID quantitation (estimated to be  $\sim 10\%$ ). However, in general the model and data are consistent.

The isotopic results for individual compounds ( $\delta^{13}\text{C}_{ij}$  and  $\Delta^{14}\text{C}_{ij}$ ) are shown graphically in Fig. 4 and 5. The model and data for the SMB pre-bomb sediment horizon (2.5–7.5 cm) is presented in Fig. 4, while the post-bomb (0–2.5 cm) model and data are shown in Fig. 5. In both figures, the  $\delta^{13}\text{C}$  model agrees within  $\pm 1\%$  of the data for all of the *n*-alkanes. The model reproduces the odd-even pattern seen in the data, showing  $^{13}\text{C}$ -enrichment in the even-numbered and  $^{13}\text{C}$ -depletion in the odd-numbered compounds. The model is offset from the data most clearly in the post-bomb sample, where it significantly under-predicts the  $\delta^{13}\text{C}$  values of the longer chain ( $\geq n\text{-C}_{29}$ ) isomers. There may be an additional,  $^{13}\text{C}$ -enriched component to the post-bomb *n*-alkanes, or the  $^{13}\text{C}$  differences between the surface and deeper sediments could represent a diagenetic effect. Another possibility is that the  $\delta^{13}\text{C}$  of one (or more) of the *n*-alkane sources has not remained uniform over time. Within the uncertainties of the model, however, the  $\delta^{13}\text{C}$  results appear to agree with the data.

The  $\Delta^{14}\text{C}$  model matches the data for all compounds measured in the pre-bomb sediments (Fig. 4). The agreement between the model and data is nearly as good for the post-bomb horizon (Fig. 5). The error associated with compound-specific  $\Delta^{14}\text{C}$  measurements is estimated to equal  $\sim \pm 20\%$  (Pearson, 2000). All of the pre-bomb model residuals were smaller than 20%, while the post-bomb residuals were slightly larger (up to 35%).

Table 2  
Results of *n*-alkane mixing model

	Fraction petroleum	Fraction Monterey shale	Fraction modern plant wax
SMB 0–2.5 cm	0.12	0.08	0.80
SMB 2.5–7.5 cm	0.05	0.08	0.87
SMB 0–2.5 cm	$\Delta^{14}\text{C}_{\text{measured}} (\text{‰})$	$\Delta^{14}\text{C}_{\text{model}} (\text{‰})$	Difference (‰)
<i>n</i> -C <sub>24+26+28+30</sub>	–741	–733	8
<i>n</i> -C <sub>27</sub>	–243	–216	27
<i>n</i> -C <sub>29</sub>	30	–5	–35
<i>n</i> -C <sub>31</sub>	–113	–89	24
SMB 2.5–7.5 cm	$\Delta^{14}\text{C}_{\text{measured}} (\text{‰})$	$\Delta^{14}\text{C}_{\text{model}} (\text{‰})$	Difference (‰)
<i>n</i> -C <sub>24+26+28+30</sub>	–617	–622	–5
<i>n</i> -C <sub>27</sub>	–223	–237	–14
<i>n</i> -C <sub>29</sub>	–122	–126	–4
<i>n</i> -C <sub>31</sub>	–170	–176	–6

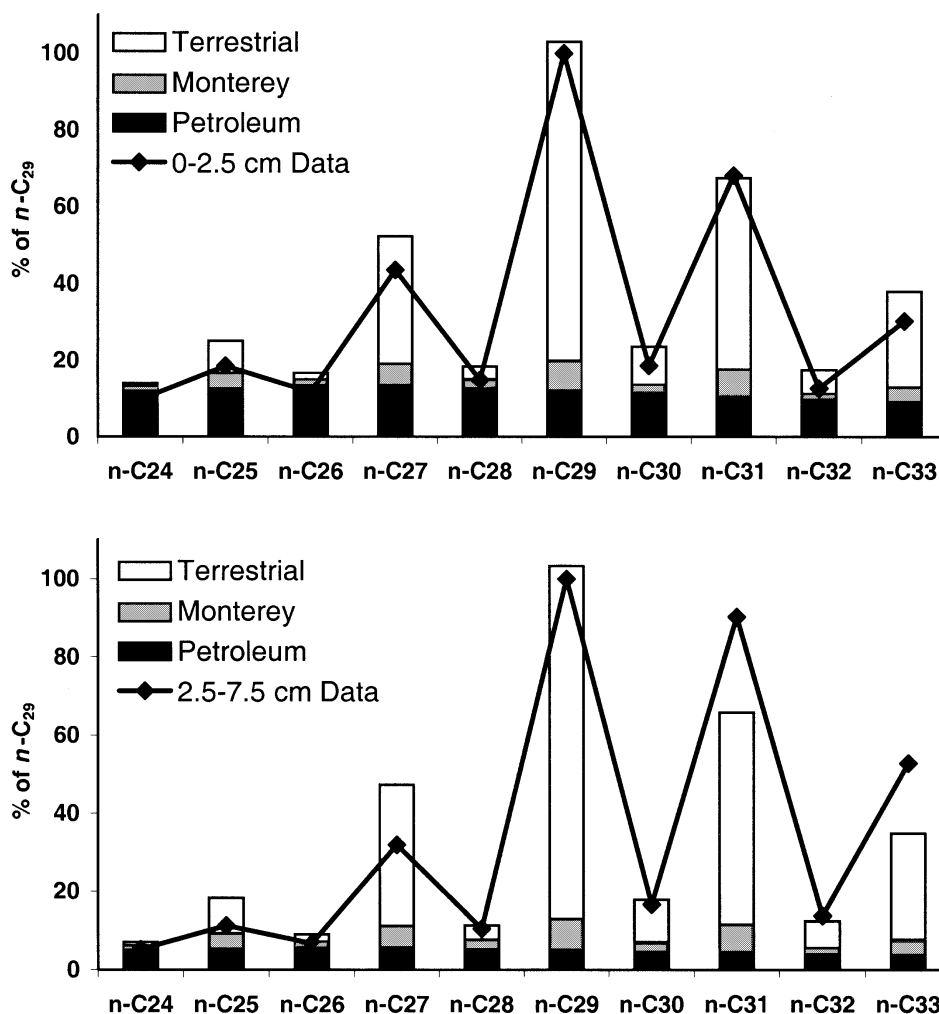


Fig. 3. Relative contributions of each of the three end members to the samples. Bars: model results for the three components. Diamonds: measured abundance in sediment relative to  $n\text{-C}_{29}$ .

However, the compounded error associated with comparing the data to the model, if the model uncertainty is also  $\pm 20\%$ , is  $\sim \pm 30\%$ . This is probably still an optimistic estimate of the true uncertainty associated with the model, and it appears that the models and data are insignificantly different.

#### 4.2. Sensitivity analysis

The primary goal of the mixing model is to simulate the compound-specific  $\Delta^{14}\text{C}$ ,  $\delta^{13}\text{C}$ , and total concentration data sets. The required assumptions are the internal concentration distributions for each end member as well as their isotopic compositions. A preliminary assessment was made of the sensitivity of the modeled concentrations to variations in mixing or compositions of the

three end members. It indicated that a wide range of mixing ratios ( $f_{\text{plantwax}}:f_{\text{petroleum}}:f_{\text{shale}}$ ) and/or minor adjustments within end members could yield model results in acceptable agreement with the data ( $\pm 10\text{--}20\%$ ). Therefore, concentration profiles alone probably are not sufficient to decouple complex source functions for sedimentary alkanes. The isotopic portions of the model, however, are more sensitive and provide much more constraint on both the end member isotopic compositions and the final mixing ratios.

In Fig. 6a and b, the average difference between the model outcome and the data is shown for a range of assumed isotopic values (both  $\delta^{13}\text{C}$  and  $\Delta^{14}\text{C}$ ) for the modern plant wax end member. This end member represents the most abundant fraction of the total sample, and therefore most strongly determines the model output. In Fig. 6a, the y-axis is constrained within



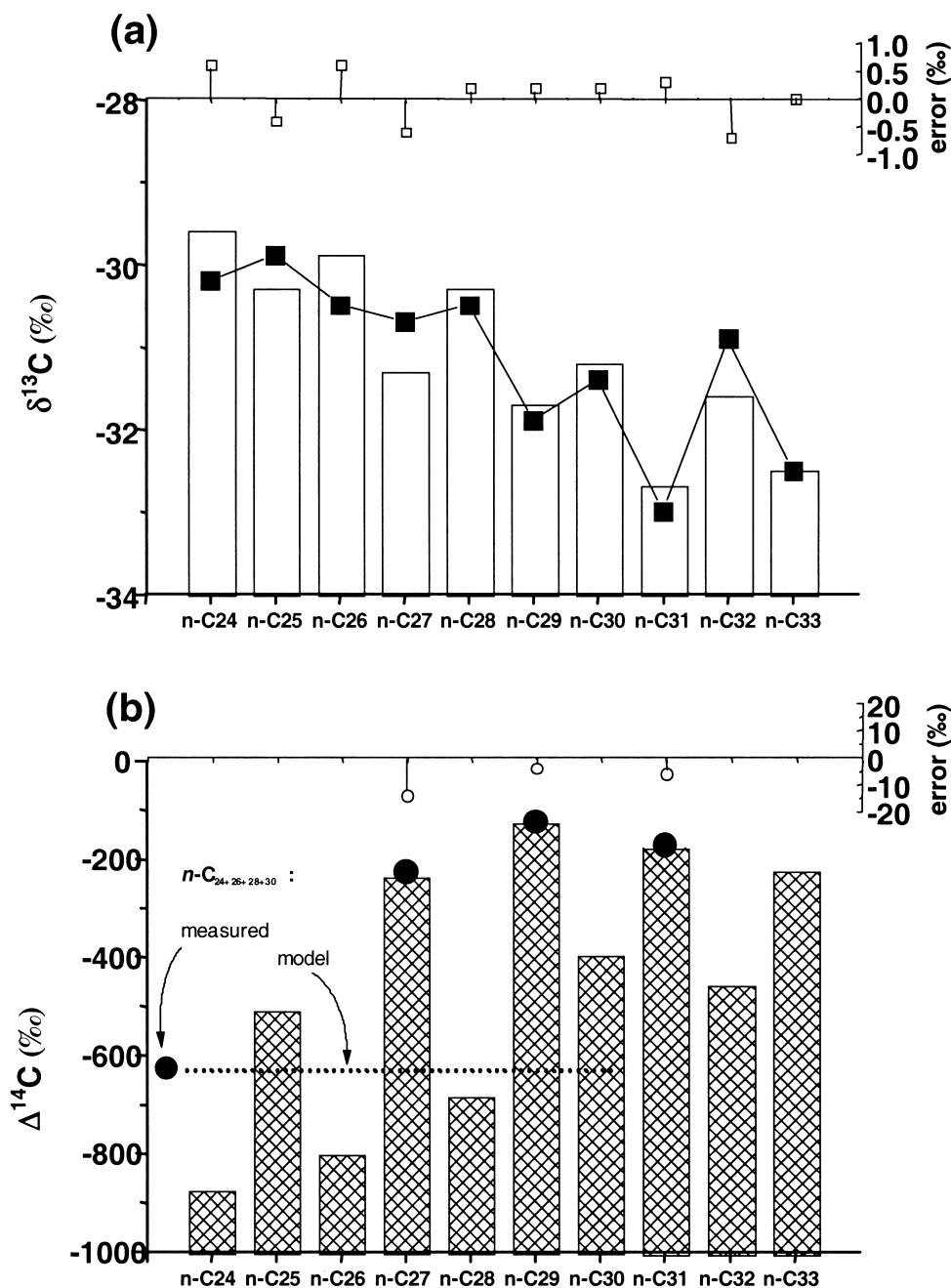


Fig. 4. Results of the mixing model for SMB pre-bomb (2.5–7.5 cm) *n*-alkanes. (a)  $\delta^{13}\text{C}$  data for *n*-C<sub>24</sub> to *n*-C<sub>33</sub> *n*-alkanes (squares) and  $\delta^{13}\text{C}$  predicted by the best-fit model solution (bars). Residuals shown above are all < 1.0‰; (b)  $\Delta^{14}\text{C}$  data for composite even numbered *n*-alkanes (*n*-C<sub>24+26+28+30</sub>), and individual *n*-C<sub>27</sub>, *n*-C<sub>29</sub>, and *n*-C<sub>31</sub> alkanes (circles) and  $\Delta^{14}\text{C}$  for all *n*-C<sub>24</sub> to *n*-C<sub>33</sub> alkanes predicted by the best-fit model solution (bars). The weighted average model result for *n*-C<sub>24+26+28+30</sub> is represented by a dotted horizontal line.

$\pm 0.4\%$  to show the range over which error in the model is indistinguishable from  $\delta^{13}\text{C}$  analytical error. This represents the “acceptable” range of disagreement between data and model. The same approach is shown

in Fig. 6b for  $\Delta^{14}\text{C}$ , this time with the *y*-axis constrained within  $\pm 30\%$  for  $^{14}\text{C}$  measurement error. Again, this was chosen as the “acceptable” range of disagreement between data and model.

Fig. 6a shows that  $\delta^{13}\text{C}$  of the terrestrial end member is (i) better constrained for the pre-bomb sample than for the post-bomb sample, and (ii) that for this pre-

bomb sample, values of  $\delta^{13}\text{C}$  beyond  $\pm 1\%$  from the values used in our model yield unacceptable results. Fig. 6b shows that the acceptable range of input values that

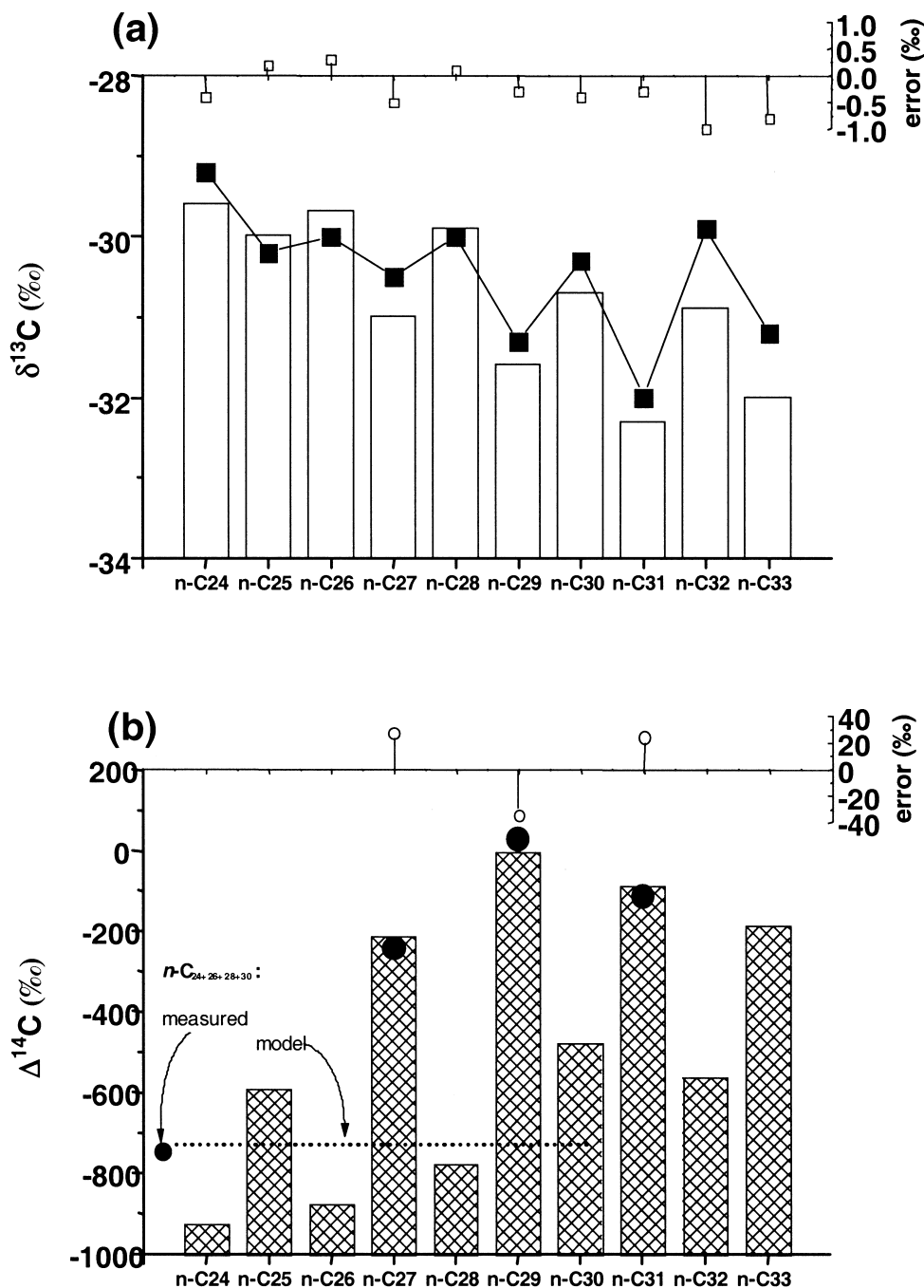


Fig. 5. Results of the mixing model for SMB post-bomb (0–2.5 cm) *n*-alkanes: (a)  $\delta^{13}\text{C}$  data for  $n\text{-C}_{24}$  to  $n\text{-C}_{33}$  *n*-alkanes (squares) and  $\delta^{13}\text{C}$  predicted by the best-fit model solution (bars). Residuals shown above are all  $< 1.0\%$ ; (b)  $\Delta^{14}\text{C}$  data for composite even numbered *n*-alkanes ( $n\text{-C}_{24+26+28+30}$ ), and individual  $n\text{-C}_{27}$ ,  $n\text{-C}_{29}$ , and  $n\text{-C}_{31}$  alkanes (circles) and  $\Delta^{14}\text{C}$  for all  $n\text{-C}_{24}$  to  $n\text{-C}_{33}$  alkanes predicted by the best-fit model solution (bars). The weighted average model result for  $n\text{-C}_{24+26+28+30}$  is represented by a dotted horizontal line.

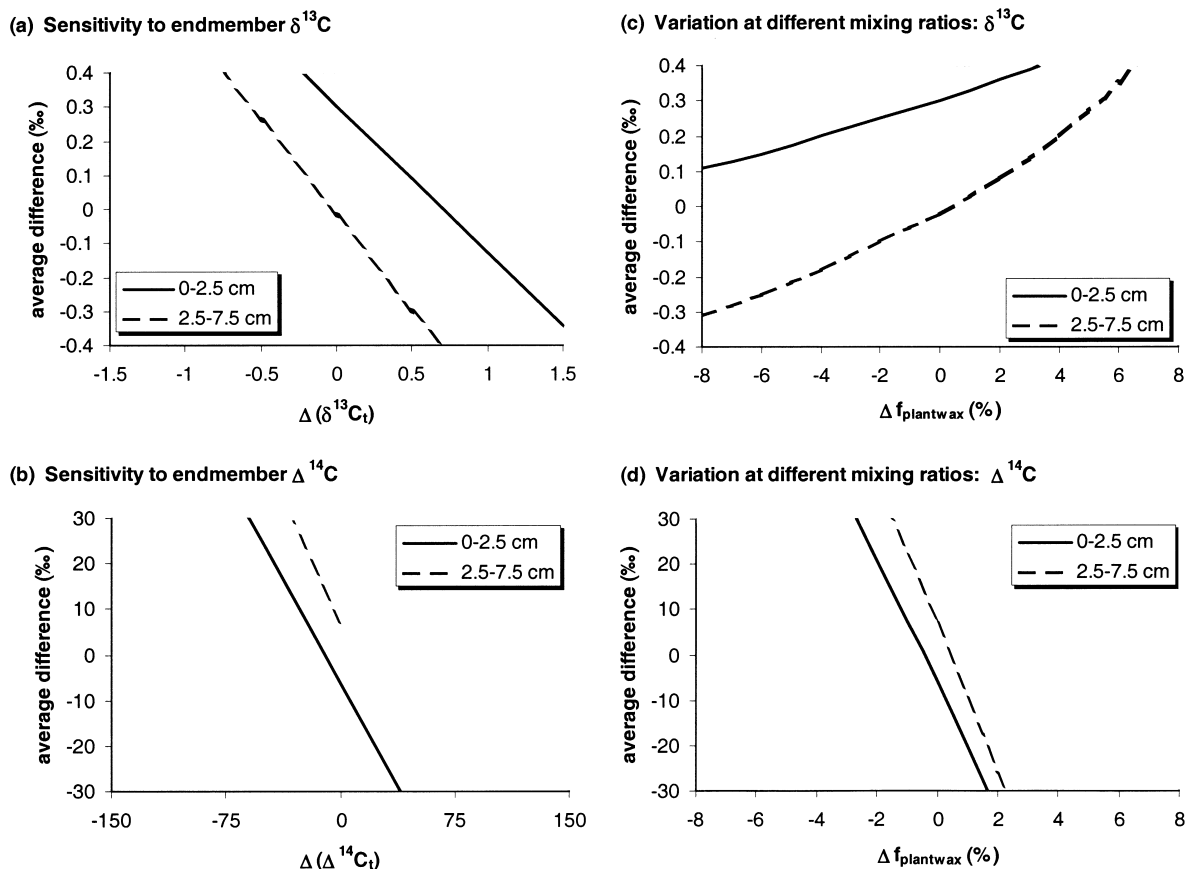


Fig. 6. Results of the sensitivity analysis. In all cases, the y-axis shows the difference between the data and the model output; only the “acceptable” range of difference is shown. The x-axis depicts the range of values tested (model input); this input is shown as its difference ( $\Delta_{\text{isotope}}$  or  $\Delta_{\text{fraction}}$ ) from the final value reported in Table 2: (a) sensitivity of the  $\delta^{13}\text{C}$  output to the  $\delta^{13}\text{C}$  value chosen for the modern plant wax end member; (b) sensitivity of the  $\Delta^{14}\text{C}$  output to the  $\Delta^{14}\text{C}$  value chosen for the modern plant wax end member; (c) sensitivity of the  $\delta^{13}\text{C}$  output to the fraction attributed to the modern plant wax end member; (d) sensitivity of the  $\Delta^{14}\text{C}$  output to the fraction attributed to the modern plant wax end member.

can be used for  $\Delta^{14}\text{C}_{\text{plantwax}}$  is very small. By definition, pre-bomb  $\Delta^{14}\text{C}$  cannot be  $>0\text{‰}$ , and the model output is unacceptable at  $\Delta^{14}\text{C}_{\text{plantwax}} < -25\text{‰}$ . For the post-bomb sample, the model is also very sensitive and produces unacceptable results outside of a  $\pm 50\text{‰}$  range of the chosen value of  $+235\text{‰}$ .

The model is more constrained in general by  $^{14}\text{C}$  than it is by  $^{13}\text{C}$ , primarily due to the larger dynamic range in  $\Delta^{14}\text{C}$  as compared to  $\delta^{13}\text{C}$  within our data set. This is apparent if the  $\delta^{13}\text{C}$  and  $\Delta^{14}\text{C}$  results of the model are examined for their sensitivity to different mixing ratios of the three components. Using our chosen end member concentrations and isotopic compositions, the dominant ( $f_{\text{plantwax}}$ ) fraction was varied by  $\pm 8\%$  ( $\pm 0.08$ ) around the final solutions from Table 2. (Mass balance was conserved by adding or subtracting carbon equally from the two fossil fractions.) Fig. 6c and d indicates that a wide range of mixtures can generate acceptable  $^{13}\text{C}$  results, but useful model output for  $^{14}\text{C}$  can be generated

only within a narrow range of mixing ratios. This is true for both the pre-bomb and post-bomb samples, thus Fig. 6d suggests that the model is significant to  $\pm 2\%$  with respect to mixing.

## 5. Discussion

The ability of these models to reproduce the  $\Delta^{14}\text{C}$  data has several implications. First, the model is able to explain the decrease in  $\Delta^{14}\text{C}$  of the even-numbered alkanes in the post-bomb sedimentary horizon. The model result for  $\text{C}_{24+26+28+30}$  was calculated by multiplying the modeled  $\Delta^{14}\text{C}$  of each even-numbered compound by the modeled total abundance of that compound. The ability of the model to generate the measured  $\Delta^{14}\text{C}$  value is especially important, because it means that both the relative fractions of the three end members and the overall concentration distributions of

the C<sub>24–30</sub> isomers are correct. The model therefore confirms the hypothesis, based on relative abundance and  $\delta^{13}\text{C}$  alone, that there is a significant fossil component to the even-numbered alkanes. It also confirms that the relative concentration of this component is higher in the surface horizon in comparison to the deeper sediments.

A second implication of the  $\Delta^{14}\text{C}$  data is that there apparently is no need to invoke an additional source of pre-aged terrestrial carbon (e.g. paleosols) to explain the isotopic results. The terrestrial plant wax end member satisfies the data using modern  $\Delta^{14}\text{C}$  values. The pre-bomb  $\Delta^{14}\text{C}_{\text{plantwax}}$  value used in the model was 0‰. The associated uncertainties in the  $\Delta^{14}\text{C}$  data alone mean the true  $\Delta^{14}\text{C}_{\text{plantwax}}$  value could easily be as low as  $-20\text{‰}$  (equivalent to  $\sim 150$  years). However, the presence of bomb  $^{14}\text{C}$  in the surface sediment sample is strong evidence for an average continental residence time of  $< 100$  years (equivalent to a pre-bomb  $\Delta^{14}\text{C} = -10\text{‰}$ ).

The calculated value for post-bomb  $\Delta^{14}\text{C}_{\text{plantwax}}$  is more difficult to interpret, because the atmospheric  $\Delta^{14}\text{C}$  record has not been constant throughout this century. The average  $\Delta^{14}\text{C}$  of atmospheric CO<sub>2</sub> between 1980 and the present is estimated to be  $\sim +200\text{‰}$  based on data in Levin and Kromer (1997). However, the SMB 0–2.5 cm sediment horizon dates to  $\sim 1960$ , and the average  $\Delta^{14}\text{C}$  of atmospheric CO<sub>2</sub> is closer to  $+400\text{‰}$  over this longer time interval. The majority of the *n*-alkanes in these samples are of terrestrial origin, and based on geochemical considerations this component apparently is resistant to degradation. This makes it unlikely that the alkanes in the 0–2.5 cm horizon are derived exclusively from products dating only from the last two decades. Instead, it is more likely that the modeled  $\Delta^{14}\text{C} = +235\text{‰}$  reflects a mixture of plant waxes derived from throughout the years 1960–1996 plus some relatively modern material dating from prior to nuclear weapons testing ( $\Delta^{14}\text{C} = 0\text{‰}$ ). A  $\Delta^{14}\text{C}$  value of  $\sim +235\text{‰}$  ( $\sim 45$  years at  $+400\text{‰}$ , plus  $\sim 30$  years at  $0\text{‰}$ ) would be consistent with an average age for the terrestrial component of  $\sim 75$  years. This is curiously (and perhaps coincidentally) close to the estimated global average 80-year residence time of carbon in the upper 1 m of soil humus (Hedges and Oades, 1997). It is also consistent with a pre-bomb  $\Delta^{14}\text{C}_{\text{plantwax}}$  value between  $-10$  and  $0\text{‰}$ .

Although modern terrestrial components dominate the SMB alkane distributions, the concentration of petroleum-derived alkanes is significantly higher in the surface sample (12%) compared to the deeper sediments (5%). It is unknown whether this is a diagenetic effect, the result of greater anthropogenic influence in the upper horizon, or a combination of both. Due to the reported presence of the Monterey oil biomarker, C<sub>28</sub> bisnorhopane, in SMB sediments, some portion of the

petroleum fraction in this environment probably derives from natural seepage (Simoneit and Kaplan, 1980). Anthropogenic sources of petroleum-derived alkanes include sewage outfall and local shipping traffic (Venkatesan and Kaplan, 1992). Sedimentary profiles of total hydrocarbons in California Borderland basin sediments show a clear increase in concentration beginning in the early to mid-1900s, presumably due to human activity (Eganhouse and Venkatesan, 1993). In SMB, the maximum concentration of polycyclic aromatic hydrocarbons occurs slightly below 2.5 cm (A. Pearson, unpubl. data), suggesting that there should be substantial anthropogenic influence on the *n*-alkanes in both samples studied here. Since the hydrocarbon sources to both horizons apparently are similar, the smaller percentage of petroleum-derived alkanes at depth may reflect differing rates of diagenesis for the petroleum, shale, and plant wax components.

The fractional contribution of shale-derived *n*-alkanes (8%) appears to remain constant. This uniformity suggests that the shale component is relatively resistant to remineralization and that it degrades, on average, at about the same rate as the total pool of hydrocarbons. This observation helps address the question of whether ancient organic carbon on the continents experiences complete oxidation or whether a fraction survives and is re-buried in marine sediments (Hedges, 1992). Our model is consistent with other studies that have suggested incomplete weathering of eroded continental materials (e.g. Barrick et al., 1980; Petsch et al., 2000). In addition, the presence of multiple fossil and modern hydrocarbon components in the SMB environment helps to explain some of the variability in  $\Delta^{14}\text{C}$  values previously reported for individual alkanes extracted from Arabian Sea sediments ( $\Delta^{14}\text{C} = -724\text{‰}$  to  $-594\text{‰}$ ) and Black Sea sediments ( $\Delta^{14}\text{C}$  range  $-158$  to  $-66\text{‰}$ ) (Eglinton et al., 1997). In contrast, autochthonous biomarkers, such as phytoplanktonic sterols, exhibit uniform  $^{14}\text{C}$  concentrations in these SMB samples ( $\Delta^{14}\text{C} = +62 \pm 23\text{‰}$ ,  $n = 18$ ; Pearson et al., 2000).

## 6. Conclusions

The algebraic mixing model used in this work was able to accurately reproduce a series of compound-specific  $\delta^{13}\text{C}$  and  $\Delta^{14}\text{C}$  measurements obtained for SMB sedimentary *n*-alkanes. The conclusions drawn from the model simulations were also consistent with hypotheses based solely on organic geochemical considerations. The majority of SMB sedimentary alkanes ( $> 80\%$ ) originate from modern terrestrial plant waxes. A smaller, constant amount (8%) derives from the weathering of fossil material having a CPI value of  $\sim 3$  and which apparently is resistant to degradation (shales or other continental rocks). The remainder of the alkanes come

from natural or anthropogenic petroleum sources, and this component is more concentrated in surface sediments.

In addition, the model confirmed that the non-fossil plant waxes delivered to SMB sediments are of very recent biosynthetic origin. For this end member,  $\Delta^{14}\text{C}$  values of  $\sim 0\text{‰}$  in the pre-bomb sample and  $>0\text{‰}$  in the post-bomb sample are both equivalent to  $<100$  years continental residence time. A fraction of allochthonous carbon with an intermediate degree of  $^{14}\text{C}$  depletion may also be contained within the SMB sediments. However, it is possible that this fraction may not contain a large hydrocarbon signal and therefore would not be addressed in the data and model presented here. One possible explanation is that the terrestrial alkanes represent the continental aerosol flux. Another more recalcitrant tracer, such as lignin, may be required to address the process of soil erosion and transport. In addition, new methods for measuring the natural abundance of deuterium (D/H ratios) in lipids may help refine the terrestrial component of biomarkers representing multiple sources (Sessions et al., 1999).

#### Acknowledgements

The authors wish to thank the NOSAMS facility staff for AMS analytical support; C. Johnson, L. Houghton, and E. Franks for  $\delta^{13}\text{C}$  analyses; and B. Benitez-Nelson for general laboratory assistance. SIO and the crew of the R/V *Roger Revelle* generously donated their time for two days of sample collection in SMB. F. Prah and B. Popp provided thorough and helpful reviews of the manuscript. This work was supported by NSF grants OCE-9415568, OCE-9809624, and OCE-9708478 to T.I.E. and by the NOSAMS-NSF cooperative agreement. A.P. also was supported by an MIT Ida Green fellowship and an EPA graduate fellowship. WHOI contribution number 10245.

Associate Editor—M. Altabet

#### References

- Barrick, R.C., Hedges, J.I., Peterson, M.L., 1980. Hydrocarbon geochemistry of the Puget Sound region — I. sedimentary acyclic hydrocarbons. *Geochimica et Cosmochimica Acta* 44, 1349–1362.
- Bird, M.I., Summons, R.E., Gagan, M.K., Roksandic, Z., Dowling, L., Head, J., Fifield, L.K., Cresswell, R.G., Johnson, D.P., 1995. Terrestrial vegetation change inferred from *n*-alkane  $\delta^{13}\text{C}$  analysis in the marine environment. *Geochimica et Cosmochimica Acta* 59, 2853–2857.
- Brassell, S.C., Eglinton, G., 1980. Environmental chemistry; an interdisciplinary subject; natural and pollutant organic compounds in contemporary aquatic environments. In: Albaiges, J. (Ed.), *Analytical Techniques in Environmental Chemistry*, Pergamon Series on Environmental Science, vol. 3, pp. 1–22.
- Clayton, C.J., Bjorøy, M., 1994. Effect of maturity on  $^{13}\text{C}/^{12}\text{C}$  ratios of individual compounds in North Sea oils. *Organic Geochemistry* 21, 737–750.
- Collister, J.W., 1992. An isotopic biogeochemical study of the Green River Oil Shale (Piceance Creek Basin, Colorado). PhD Dissertation, Indiana University.
- Collister, J.W., Rieley, G., Stern, B., Eglinton, G., Fry, B., 1994a. Compound-specific  $\delta^{13}\text{C}$  analyses of leaf lipids from plants with differing carbon dioxide metabolisms. *Organic Geochemistry* 21, 619–627.
- Collister, J.W., Lichtfouse, E., Hieshima, G., Hayes, J.M., 1994b. Partial resolution of sources of *n*-alkanes in the saline portion of the Parachute Creek Member, Green River Formation (Piceance Creek Basin, Colorado). *Organic Geochemistry* 21, 645–659.
- Eganhouse, R.P. & Venkatesan, M.I. 1993. Chemical Oceanography and Geochemistry, In: Dailey, M.D., Reish, D.J., Anderson, J.W. (Eds.), *Ecology of the Southern California Bight, a Synthesis and Interpretation*. University of California Press, Berkeley, pp. 71–171.
- Eglinton, G., Gonzales, A.G., Hamilton, R.J., Raphael, R.A., 1962. Hydrocarbon constituents of the wax coating of plant leaves: a taxonomic survey. *Phytochemistry* 1, 89–102.
- Eglinton, T.I., Aluwihare, L.I., Bauer, J.E., Druffel, E.R.M., McNichol, A.P., 1996. Gas chromatographic isolation of individual compounds from complex matrices for radiocarbon dating. *Analytical Chemistry* 68, 904–912.
- Eglinton, T.I., Benitez-Nelson, B.C., Pearson, A., McNichol, A.P., Bauer, J.E., Druffel, E.R.M., 1997. Variability in radiocarbon ages of individual organic compounds from marine sediments. *Science* 277, 796–799.
- Gagosian, R.B., Peltzer, E.T., Zafiriou, O.C., 1981. Atmospheric transport of continentally-derived lipids in aerosols to the tropical North Pacific. *Nature* 291, 312–314.
- Hayes, J.M., Freeman, K.H., Popp, B.N., Hoham, C.H., 1990. Compound-specific isotopic analyses: A novel tool for reconstruction of ancient biogeochemical processes. *Organic Geochemistry* 16, 1115–1128.
- Hedges, J.I., 1992. Global biogeochemical cycles: progress and problems. *Marine Chemistry* 39, 67–93.
- Hedges, J.I., Oades, J.M., 1997. Comparative organic geochemistries of soils and marine sediments. *Organic Geochemistry* 27, 319–361.
- Levin, I., Kromer, B., 1997. Twenty years of atmospheric  $^{14}\text{CO}_2$  observations at Schauinsland. *Radiocarbon* 39, 205–218.
- Lichtfouse, E., Eglinton, T.I., 1996.  $^{13}\text{C}$  and  $^{14}\text{C}$  evidence of pollution of a soil by fossil fuel and reconstruction of the composition of the pollutant. *Organic Geochemistry* 23, 969–973.
- Lockheart, M.J., van Bergen, P.F., Evershed, R.P., 1996. Variations in the stable carbon isotope compositions of individual lipids from the leaves of modern angiosperms: implications for the study of higher land plant-derived sedimentary organic matter. *Organic Geochemistry* 26, 137–153.
- Pearson, A., 2000. Biogeochemical Applications of Compound-Specific Radiocarbon Analysis. PhD Thesis, Massachusetts Institute of Technology/Woods Hole Oceanographic Institution, USA.

- Pearson, A., McNichol, A.P., Schneider, R.J., von Reden, K.F., 1998. Microscale AMS  $^{14}\text{C}$  measurement at NOSAMS. *Radiocarbon* 40, 61–76.
- Pearson, A., Eglinton, T.I., McNichol, A.P., 2000. An organic tracer for surface ocean radiocarbon. *Paleoceanography*, accepted.
- Petsch, S.T., Berner, R.A., Eglinton, T.I., 2000. A field study of the chemical weathering of ancient sedimentary organic matter. *Organic Geochemistry* 31, 475–487.
- Prahl, F.G., Muehlhausen, L.A., Lyle, M., 1989. An organic geochemical assessment of oceanographic conditions at MANOP Site C over the past 26,000 years. *Paleoceanography* 4, 495–510.
- Prahl, F.G., Ertel, J.R., Goñi, M.A., Sparrow, M.A., Ever-smeyer, B., 1994. Terrestrial organic carbon contributions to sediments on the Washington margin. *Geochimica et Cosmochimica Acta* 58, 3035–3048.
- Reddy, C.M., Eglinton, T.I., Palic, R., Benitez-Nelson, B.C., Stojanovic, G., Palic, I., Stankovic, S., Eglinton, G., 1999. Even carbon number predominance of plant wax *n*-alkanes: a correction. *Organic Geochemistry* 31, 331–336.
- Sakata, S., Hayes, J.M., McTaggart, A.R., Evans, R.A., Lekrone, K.J., Togasaki, R.K., 1997. Carbon isotopic fractionation associated with lipid biosynthesis by a cyanobacterium: Relevance for interpretation of biomarker records. *Geochimica et Cosmochimica Acta* 24, 5379–5389.
- Schneider, J.K., Gagosian, R.B., 1985. Particle size distribution of lipids in aerosols off the coast of Peru. *J. Geophysical Research* 90, 7889–7898.
- Schouten, S., 1995. Structural and Stable Carbon Isotope Studies of Lipids in Immature Sulphur-rich Sediments. PhD Thesis, University of Groningen, The Netherlands.
- Sessions, A.L., Burgoyne, T.W., Schimmelmann, A., Hayes, J.M., 1999. Fractionation of hydrogen isotopes in lipid biosynthesis. *Organic Geochemistry* 30, 1193–1200.
- Simoneit, B.R.T., Kaplan, I.R., 1980. Triterpenoids as molecular indicators of paleoseepage in recent sediment off the Southern California Bight. *Marine Environmental Research* 3, 113–128.
- Stuiver, M., Polach, H.A., 1977. Discussion: reporting of  $^{14}\text{C}$  data. *Radiocarbon* 19, 355–363.
- Tissot, B.P., Welte, D.H., 1984. *Petroleum Formation and Occurrence*, 2nd Edition. Springer.
- Venkatesan, M.I., Kaplan, I.R., 1992. Vertical and lateral transport of organic carbon and the carbon budget in Santa Monica Basin, California. *Progress in Oceanography* 30, 291–312.
- Volkman, J.K., Johns, R.B., Gillan, F.T., Perry, G.J., Bavor Jr., H.J., 1980. Microbial lipids of an intertidal sediment — I. Fatty acids and hydrocarbons. *Geochimica et Cosmochimica Acta* 44, 1133–1143.
- von Reden, K.F., Schneider, R.J., McNichol, A.P., Pearson, A., 1998.  $^{14}\text{C}$  AMS measurements of < 100 mg samples with a high-current system. In: Mook, W.G., Van der Plicht, J. (Eds.), *Proceedings of the 16th International  $^{14}\text{C}$  conference*. *Radiocarbon* 40, pp. 247–253.
- Wilhelms, A., Larter, S.R., Hall, K., 1994. A comparative study of the stable carbon isotopic composition of crude oil alkanes and associated crude oil asphaltene pyrolysate alkanes. *Organic Geochemistry* 21, 751–759.